CONF-930159--7

Competition among autoionization, predissociation, and ion-pair formation in molecular hydrogen

J. L. Dehmer, P. M. Dehmer, S. T. Pratt, and E. F. McCormack
Argonne National Laboratory
Argonne, IL 60439 U.S.A.

ANL/ER/CP--78668

DE93 006759

ABSTRACT

We have investigated autoionization, predissociation, and ion-pair formation from highly excited states of molecular hydrogen by using double-resonance excitation via the E,F $^1\Sigma_g^+$, v=6 level. The energetic threshold for ion-pair formation occurs just below the H_2^+ X $^2\Sigma_g^+$, v^+=9 ionization threshold. The spectrum in this region was studied by using conventional and constant-ionic-state photoelectron spectroscopy, by monitoring the H^- production, and by detecting dissociation products by ionization with a third laser. The decay dynamics in this region are extremely rich, because the excited levels may decay by rotational and vibrational autoionization, by predissociation to neutral H + H* (n=2,3,4), by predissociation to the ion pair $H^+ + H^-$, and by fluorescence. In addition, the dissociative potential curve of the $2p\sigma_u 3s\sigma_g$ $^1\Sigma_u^+$ doubly excited electronic state crosses the H_2^+ X $^2\Sigma_g^+$ potential curve in the same energy region, and the electronic autoionization of this state is found to significantly influence these decay processes.

1. INTRODUCTION

Laser techniques have greatly expanded our ability to prepare and interrogate excited molecular complexes in order to investigate questions of molecular spectroscopy and dynamics that lay beyond our reach just a few years ago. Of particular interest here is the selective preparation of well-characterized excited molecular states and the observation by photoelectron and mass spectrometry of alternative decay products as a function of the energy placed in different rovibronic modes. This affords us the opportunity to study the interplay of electronic and nuclear modes in molecular fields at the quantum state specific level and, thus, to gain insight into fundamental mechanisms of molecular physics and chemistry.

Here we briefly summarize a series of studies in which we used double-resonance excitation via the E,F $^1\Sigma_g^+$, v=6 level to populate Rydberg levels converging to the H_2^+ X $^2\Sigma_g^+$, v^+=9 ionization threshold. These levels can be viewed as reaction intermediates that can decay into several different types of products, as shown schematically in Fig. 1. In the center of Fig. 1, the Rydberg states are represented by $H_2^*(v, N)$. To the right are indicated the ion-pair and the three energetically allowed dissociation decay channels. The decay paths on the right-hand side of Fig. 1 represent the decay of the Rydberg complex by means of conversion of electronic to vibrational (translational) energy. The decay channels to the left of Fig. 1, on the other hand, represent decay by conversion of rovibrational energy to electronic energy (ionization). Specifically, decay by rotational autoionization, vibrational ionization, and electronic autoionization are shown, right to left. Therefore, the excited complex in Fig. 1 represents a rich microcosm of basic molecular mechanisms. Furthermore, the processes discussed here are also related to associative ionization, ion neutralization, and dissociative recombination in hydrogen, which have important applications in gaseous electronics and astrophysics.

Figure 2 shows the potential energy curves that are relevant to the present study. There we see the H_2^+ ionic curve, with the v^+=9 vibrational level indicated. Rydberg series with potential energy curves very similar to this will converge to each rotational and vibrational level of the ion. Rotational and vibrational autoionization will proceed when the Rydberg states converging to v^+=9

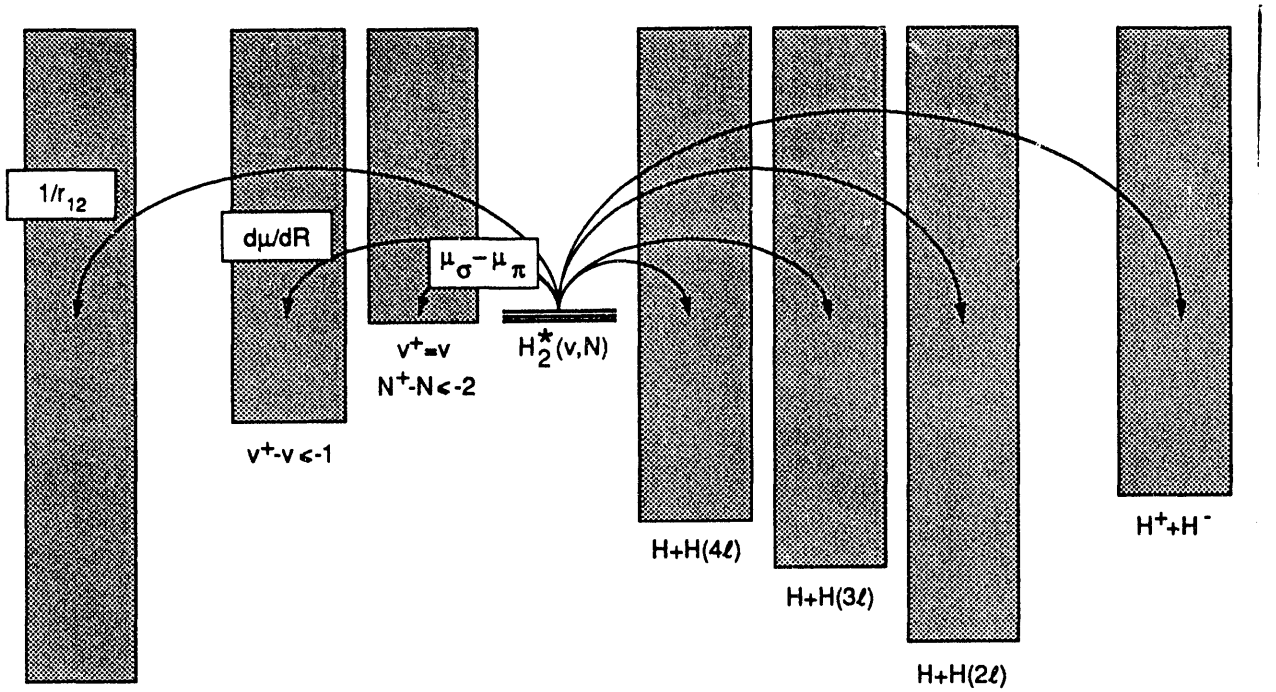

Figure 1. Schematic diagram of decay channels available to the Rydberg states converging to $H_2^+ X\ ^2\Sigma_g^+$, $v^+=9$.

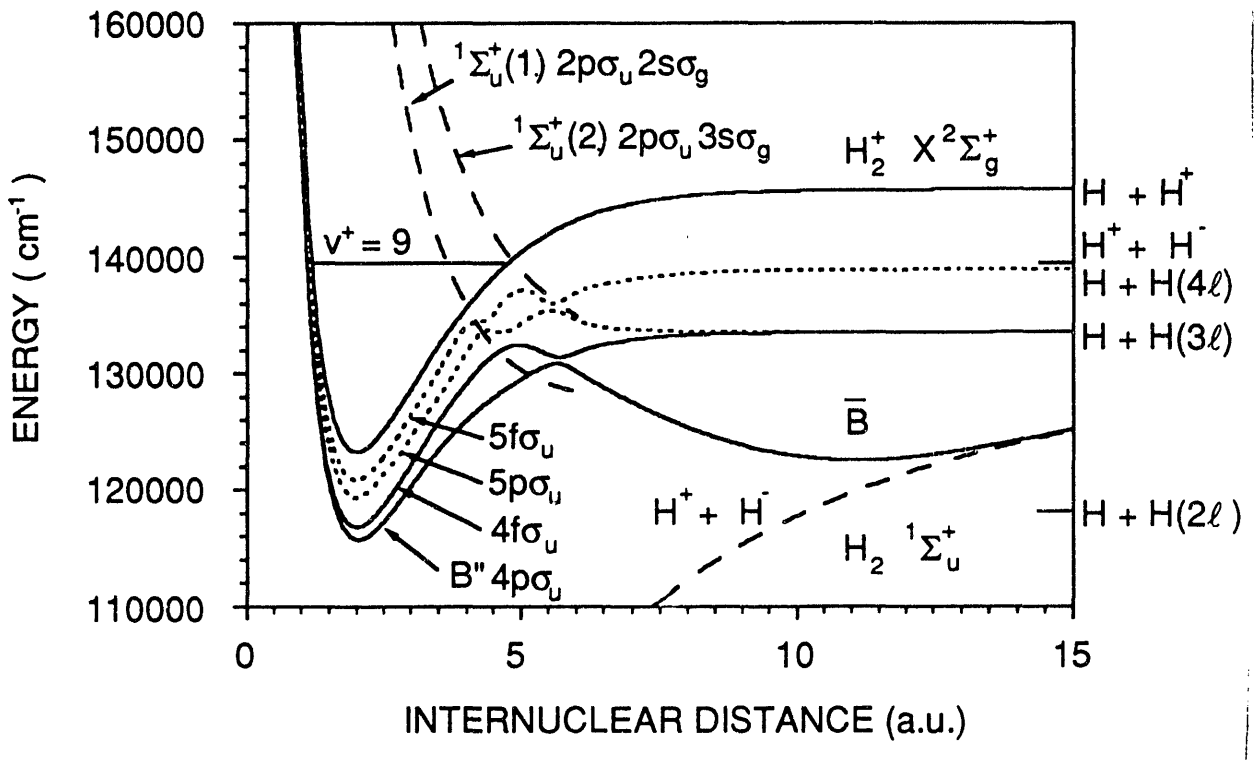

Figure 2. Relevant potential energy curves in the region of interest, taken from Refs. 1-3.

convert rotational excitation or vibrational excitation, respectively, into the energy needed to ionize the loosely bound Rydberg electron. Also shown in Fig. 2 are the ion-pair and dissociation limits that are energetically accessible for the decay of the Rydberg states converging to the $v^+=9$ ionization limit. Two doubly excited states are shown as are states that participate in the propagation of the Rydberg states and doubly excited states to the ion-pair and dissociation limits.

2. PHOTOIONIZATION

Two different types of photoelectron measurements have been performed.[4] In the first, constant-ionic-state (CIS) spectroscopy was used to determine the wavelength dependence of photoelectron intensity corresponding to different values of v^+. Monitoring photoelectrons with high values of v^+ reduces the contribution of direct ionization and thus enhances the resonant structure relative to the continuum background. For example, when photoelectrons with $v^+=8$ are monitored, the contribution to the spectrum from autoionization of $v'\geq 9$ Rydberg states is strong (because of the $\Delta v=-1$ propensity rule),[5-7] while the contribution to the spectrum from direct ionization is weak (since direct ionization of the E,F $^1\Sigma_g^+$, $v=6$ intermediate state produces very little $v^+=8$).[8] The comparison of CIS spectra obtained by monitoring photoelectrons with different values of v^+ also provides information on the autoionization mechanisms. In the second type of photoelectron measurement, these mechanisms are explored in even greater detail by recording the complete photoelectron spectra at selected wavelengths of interest.

Figure 3 shows the CIS spectrum obtained by pumping the Q(0) E,F $^1\Sigma_g^+$, $v=6 \leftarrow$ X $^1\Sigma_g^+$, $v''=0$ transition and probing the transitions to levels in the region of the $v^+=9$ threshold while monitoring the $v^+=8$ photoelectrons. As expected, this spectrum is dominated by resonant transitions to Rydberg series converging to the X $^2\Sigma_g^+$, $v^+\geq 9$ limits. Because the inner well of the E,F $^1\Sigma_g^+$ state is best described by the $1s\sigma_g 2s\sigma_g$ configuration, the dominant probe transitions are to ($\tilde{X}$ $^2\Sigma_g^+$)np Rydberg series. For the Q(0) pump transition, two Rydberg series that converge to the X $^2\Sigma_g^+$, $v^+=9$ ionization threshold are allowed. These correspond to the (X $^2\Sigma_g^+$)np, $v'=9$, $N'=0$ and (X $^2\Sigma_g^+$)np, $v'=9$, $N'=2$ series, which converge to the X $^2\Sigma_g^+$, $v^+=9$, $N^+=0$ and 2 limits, respectively. These two series may be denoted R(0)np0, $v'=9$ and R(0)np2, $v'=9$. Low-lying members of the analogous series with $v'\geq 10$ can also be observed in the wavelength region of Fig. 3.

Between 139750 and 139850 cm^{-1}, Fig. 3 displays a single, intense series, which converges to the $N^+=2$ threshold and clearly corresponds to the R(0)np2, $v'=9$ series. This series is also quite strong in the ion-pair spectrum discussed below. The X $^2\Sigma_g^+$, $v^+=9$, $N^+=0$ threshold is at 139831.135 cm^{-1}.[9-11] In the energy region above 139750 cm^{-1}, the R(0)np0, $v'=9$ series produces a quasicontinuum that does not appear to affect the regularity of the R(0)np2, $v'=9$ series; however, below 139750 cm^{-1}, the R(0)np2, $v'=9$ series is more irregular because of perturbations by members of the R(0)np0, $v'=9$ series and by interloping members of other series. It is still possible to extrapolate the R(0)np2, $v'=9$ series to lower energies, and most of the major features fall reasonably well into this series. However, the assignments at lower energies must be considered more tentative.

The photoelectron spectrum of H_2 obtained after single-color, two-photon-resonant, three-photon ionization via the E,F $^1\Sigma_g^+$, $v=6 \leftarrow$ X $^1\Sigma_g^+$, $v''=0$ transition has been reported in several previous studies.[8,12,13] Because of the $v=2$ Rydberg character of the inner-well portion of the E,F $^1\Sigma_g^+$, $v=6$ level, the photoelectron spectrum is strongly peaked at $v^+=2$, with the $v^+=1$, 2, 3, and 4 bands containing approximately 13%, 42%, 12%, and 12% of the total intensity, respectively.[8,13] None of the remaining bands contains more than 5% of the total intensity, except for the $v^+=13$ band, which is enhanced by ionization from the outer well of the E,F $^1\Sigma_g^+$ state and contains approximately 7% of the total intensity.[8,13] If the branching ratios are renormalized to include only the $v^+=0$-9 ionization continua, the $v^+=7$, 8, and 9 bands all contain less than 3% of the total intensity.

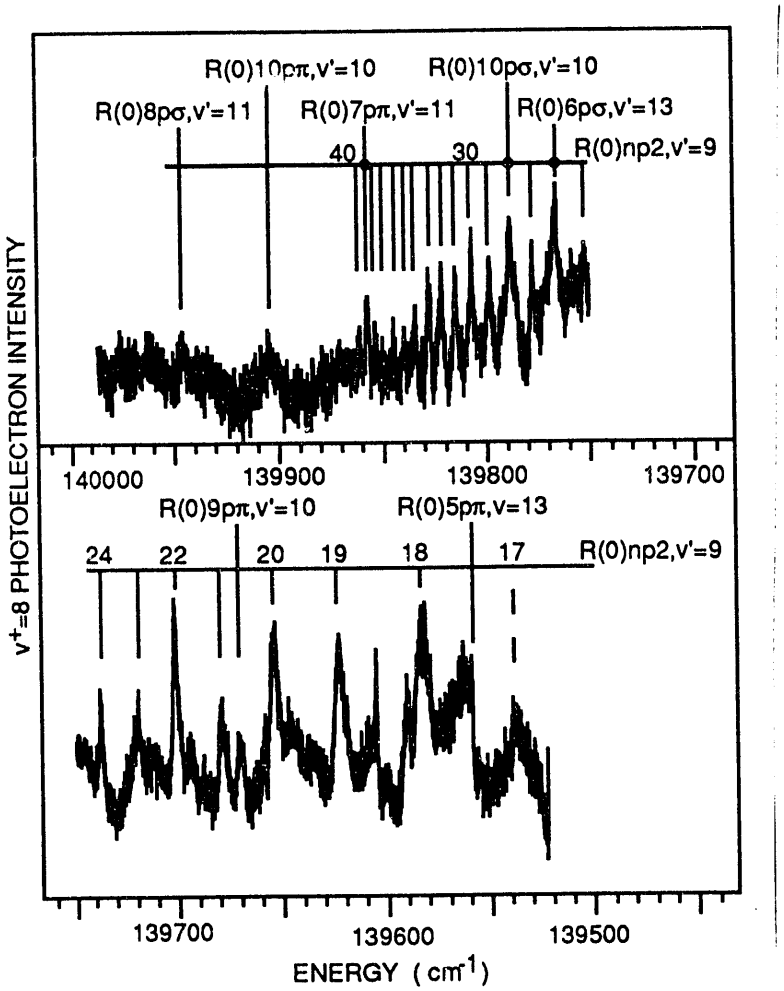

Fig. 3. The CIS spectrum obtained by pumping the two-photon Q(0) E,F $^1\Sigma_g^+$, v=6 ← X $^1\Sigma_g^+$, v"=0, transition, scanning the probe laser, and monitoring the H_2^+ X $^2\Sigma_g^+$, v^+=8 photoelectron band. The energy is with respect to the X $^1\Sigma_g^+$, v"=0, J"=0 level.

Figure 4 shows typical two-color photoelectron spectra for the Q(1) E,F $^1\Sigma_g^+$, v=6 ← X $^1\Sigma_g^+$, v"=0 pump transition with the probe laser tuned in the region just below the H_2^+ $^2\Sigma_g^+$, v^+=9 ionization threshold. Figure 4a corresponds to a total energy of 139796.3 cm^{-1}, which is between two resonances in the wavelength spectrum; Fig. 4b corresponds to the peak of the R(1)22p3, v'=9 resonance at a total energy of 139799.5 cm^{-1}. In both spectra the v^+=7 and 8 bands are significantly more intense than the corresponding bands in the single-color photoelectron spectrum. In general, the summed branching ratio for the v^+=7 and 8 bands in spectra obtained throughout this region of the spectrum is ~0.15; this is ~3 times greater than that of the single-color photoelectron spectrum. In contrast, the v^+=5 and 6 photoelectron bands are comparable in intensity in the single-color and two-color spectra. In addition to this overall difference in the appearances of the one- and two-color photoelectron spectra, Fig. 4 clearly indicates that the two-color photoelectron spectra display a significant wavelength dependence, reflecting the resonant structure in the excitation spectrum.

Because the one- and two-color photoelectron spectra were recorded by photoionization of the same intermediate level, the observed differences in the vibrational branching ratios must be due to

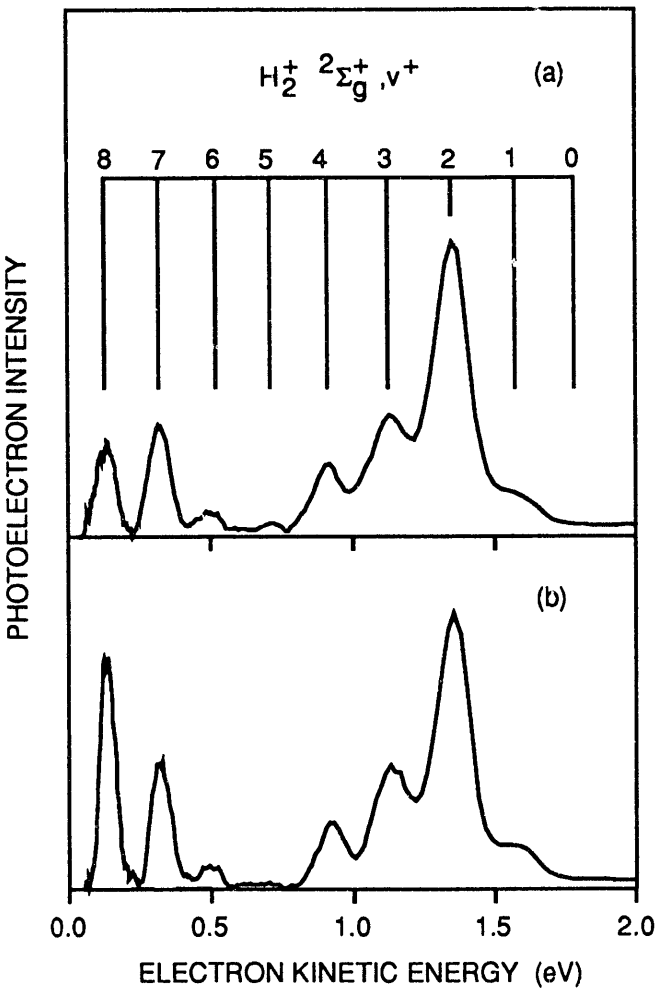

Figure 4. Photoelectron spectra obtained after two-color ionization via the E,F $^1\Sigma_g^+$, v=6, J=1 level. (a) Off-resonance spectrum at a total energy of 139976.3 cm^{-1}. (b) On-resonance spectrum at 139799.5 cm^{-1}, corresponding to the R(1)22p3, v'=9 transition.

the final state. Two-color photoionization via the E,F $^1\Sigma_g^+$, v=6 level in the energy region just below the v^+=9 threshold is expected to be affected by the resonant structure produced by Rydberg states converging to the $v^+\geq 9$ ionization thresholds. These resonances decay by vibrational autoionization and by predissociation, and they are expected to be relatively sharp. Thus, as discussed in more detail below, these resonances will influence the detailed wavelength dependence of the vibrational branching ratios; however, they probably are not responsible for the relatively high intensity of the v^+=7 and 8 photoelectron bands that is generally observed throughout the region of the present study.

Figure 2 shows that the $^1\Sigma_u^+(2)$ potential curve crosses the X $^2\Sigma_g^+$ potential curve at an energy just above the v^+=9 level. Although the vibrational overlap between the inner well of the E,F $^1\Sigma_g^+$, v=6 level and the doubly excited states is negligible near the X $^2\Sigma_g^+$, v^+=9 ionization threshold, excitation from the outer well of the E,F $^1\Sigma_g^+$, v=6 level is expected to have a more favorable

vibrational overlap and thus to produce observable consequences in the photoelectron spectrum. The large widths of the $^1\Sigma_u^+$ doubly excited states are also expected to influence the observed branching ratios over a broad energy range. This assumption is consistent with the observation of the unexpectedly high intensity of the X $^2\Sigma_g^+$, v^+=7, 8 photoelectron bands over a relatively large energy region near the v^+=9 limit. The electronic transition from the $(1s\sigma_g 2s\sigma_g)$ inner well of the E,F $^1\Sigma_g^+$ state to the $(2p\sigma_u 2s\sigma_g)$ $^1\Sigma_u^+(1)$ state is fully allowed, and the transition moment is expected to be large. The corresponding transitions to the $(2p\sigma_u 3s\sigma_g)$ $^1\Sigma_u^+(2)$ and $(2p\sigma_u 3d\pi_g)$ $^1\Pi_u(1)$ states are two-electron transitions, which are nominally forbidden. However, the $^1\Sigma_u^+(2)$ state is expected to contain some $(2p\sigma_u 2s\sigma_g)$ character, and the transition may gain intensity in that manner. The outer well of the E,F $^1\Sigma_g^+$ state has the nominal configuration $(2p\sigma_u)^2$, from which transitions to all three doubly excited states are allowed.

Using the δ-function approximation for the Franck-Condon overlap, an examination of the region of R sampled by the E,F $^1\Sigma_g^+$, v=6 wavefunction indicates that autoionization of the $^1\Sigma_u^+(1)$ state is more likely to populate lower lying vibrational levels (e.g., v^+=4, 5, 6) than the v^+=7 and 8 levels. However, because the $^1\Sigma_u^+(2)$ state crosses the ionic curve at the energy of the v^+=9 level, autoionization of this state is expected to populate the v^+=7 and 8 levels. The same is true for the $^1\Pi_u$ state, although its smaller autoionization width may reduce its contribution. Thus, it appears that the $^1\Sigma_u^+(2)$ doubly excited state is the most likely cause of the observed effects, although the $^1\Pi_u(1)$ state may contribute to some extent. Note that just below the X $^2\Sigma_g^+$, v^+=9, N^+=0 threshold, autoionization of the quasicontinuum of the R(0)np0, v'=9 series of autoionizing levels may also enhance the v^+=8 continuum.

The dramatic increase of the relative intensity of the v^+=8 band in Fig. 4b (on resonance) with respect to Fig. 4a (off resonance) is consistent with the propensity rule for vibrational autoionization.[5-7] This behavior (i.e., the increased intensity of the v^+=8 band on resonance) appears to be general throughout the region to the X $^2\Sigma_g^+$, v^+=9, N^+=J^+ threshold. As indicated by the CIS spectrum of Fig. 3, the resonant structure is most clearly reflected in the v^+=8 bands. Although the corresponding v^+=7 CIS spectra do show resonant structure analogous to that observed in the v^+=8 CIS spectra, the intensities of the resonant features are considerably weaker, and the background continuum is larger than in the former spectra. The intensity of the v^+=5 and 6 photoelectron bands is small throughout this region. In summary, both electronic and vibrational autoionization appear to play a strong role in determining the photoionization dynamics in this region of the spectrum.

3. ION-PAIR FORMATION

Figure 5 shows the H^- spectrum[14] obtained by pumping the Q(0) E,F $^1\Sigma_g^+$, v=6 ← X $^1\Sigma_g^+$, v"=0 transition and scanning in the region of the threshold for ion-pair formation. The spectra were recorded by using a delayed, pulsed electric field to extract the H^-, so that the spectra display the field-free structure. Although the same series are observed as in the CIS spectrum of Fig. 3, the intensities are quite different. Figure 6 displays a small portion of the v^+=8 CIS and H^- spectra together. The overall intensity of the H^- signal is a small fraction of a percent of that of the v^+=8 CIS signal, reflecting the weak nature of the ion-pair process. Figure 6 clearly shows strong variations in the relative intensities and profiles of the two decay pathways, as some features appear as peaks in both spectra whereas others appear as peaks in the CIS spectrum and dips in the H^- spectrum. This variation must result from the complex interactions among the initially excited Rydberg states and the singly and doubly excited predissociative states at small R as well as from the crossings and avoided crossings in the intermediate-R region (10-270 a.u.). A detailed understanding of the dynamics of ion-pair formation must await detailed theoretical calculations. These might best be performed within the framework of multichannel quantum defect theory (MQDT).

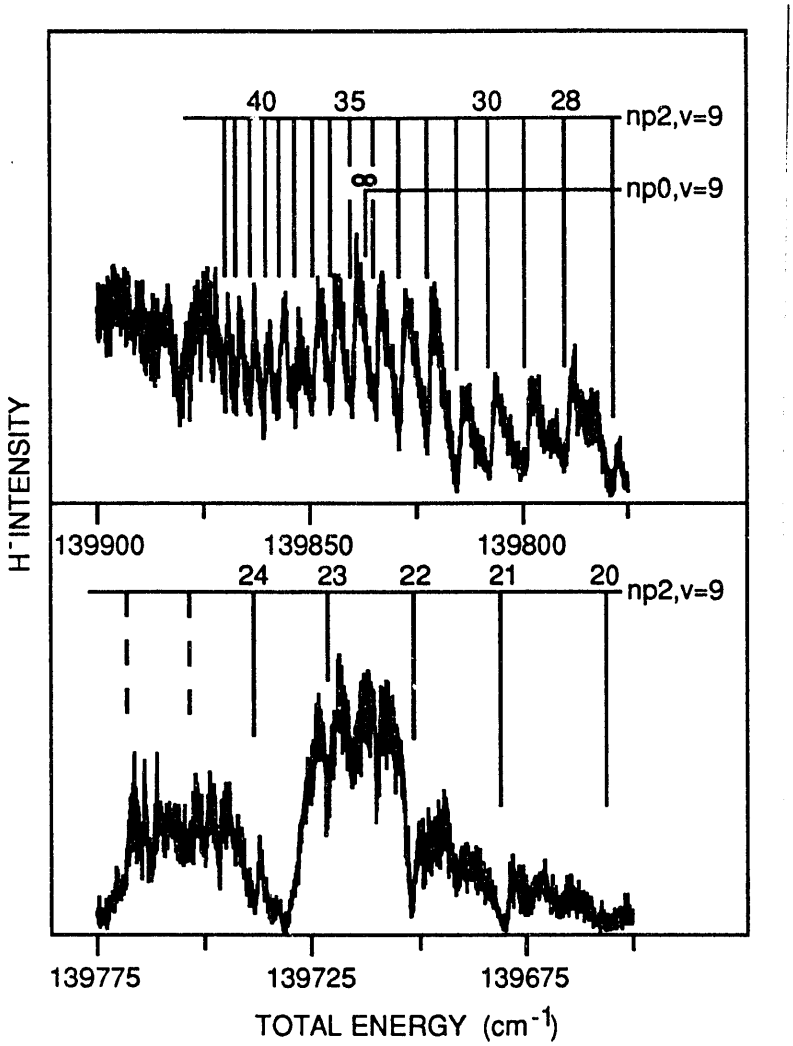

Figure 5. A portion of the field-free excitation spectrum for ion-pair formation obtained by pumping the Q(0) E,F $^1\Sigma_g^+$, v'=6 ← X $^1\Sigma_g^+$, v"=0 transition. The total energy is with respect to the X $^1\Sigma_g^+$, v"=0, J"=0 level.

4. DISSOCIATION

The decay of the (X $^2\Sigma_g^+$) np, v' ≥ 9 Rydberg states into the H(1s) + H(3ℓ) and H(1s) + H(4ℓ) dissociation continuua has been investigated recently.[15] The (X $^2\Sigma_g^+$) np, v ≥ 9 Rydberg states were excited by double-resonance excitation via the E,F $^1\Sigma_g^+$, v=6, J=0 and 1 states. H(3ℓ) and H(4ℓ) dissociation fragments were detected by collection of the electrons produced by nonresonant ionization in a magnetic-bottle electron spectrometer. In the energy region between the H(1s) + H(4ℓ) dissociation threshold and the X $^2\Sigma_g^+$, v$^+$=9 ionization threshold, evidence of both direct and indirect dissociation involving both singly and doubly excited electronic states is observed. Comparisons to the previously observed (X $^1\Sigma_g^+$) v$^+$=8 CIS spectrum and ion-pair spectrum reveal strong competition between the ionization and dissociation processes through both rovibrational and electronic interactions.

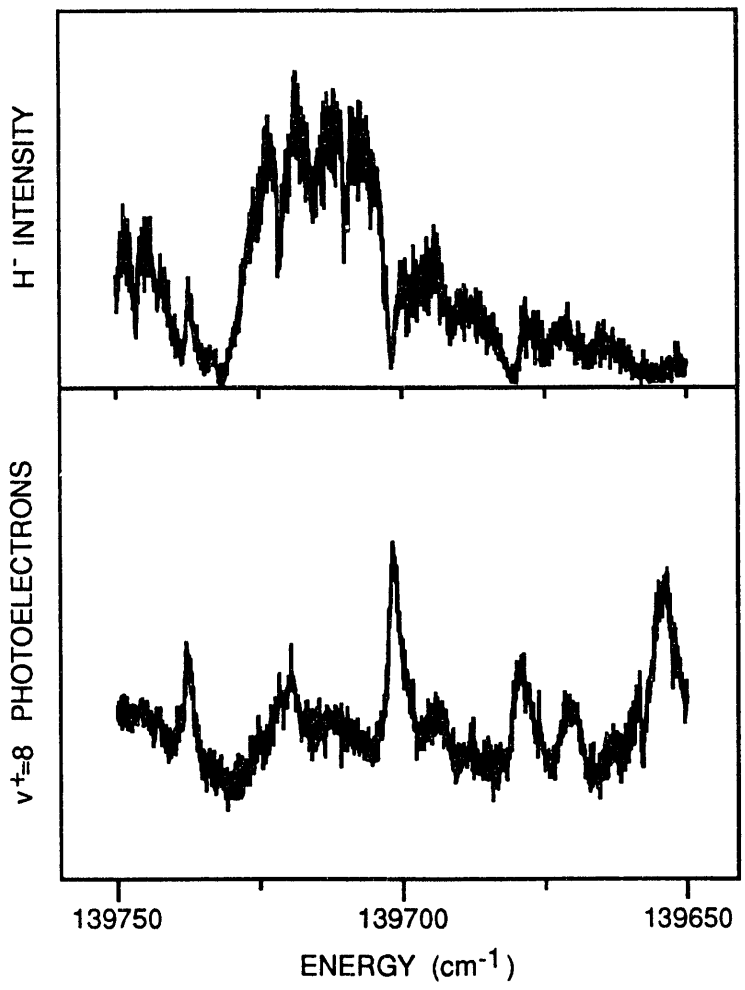

Figure 6. A portion of the $v^+=8$ CIS spectrum of Fig. 3 plotted with the corresponding portion of the H^- spectrum of Fig. 5.

The new dissociation spectra along with the previously obtained ($X\ ^1\Sigma_g^+$) $v^+=8$ CIS spectra and ion-pair spectra provide a unique set of experimental data on the decay of excited molecular hydrogen into four separate final-state continua in a common energy region. Since these results establish a picture of the decay dynamics of H_2 in an energy regime where both dissociation and ionization can occur, they can serve as an important test for theoretical approaches that attempt to account for the competition between these processes. In addition, the energy dependence of the branching ratios to the ionization and dissociation product states of the ($X\ ^2\Sigma_g^+$) np, $v' \geq 9$ Rydberg states, viewed as collision complexes, contributes to our understanding of basic chemical dynamics.

5. ACKNOWLEDGEMENTS

This work was supported by the U.S. Department of Energy, Office of Energy Research, Office of Health and Environmental Research, under Contract W-31-109-Eng-38.

6. REFERENCES

1. S. L. Guberman, "The doubly excited autoionizing states of H_2," *J. Chem. Phys.* 78, 1404-1413 (1983).

2. D. M. Bishop and R. W. Wetmore, "Vibrational spacings for H_2^+, D_2^+, and H_2," *Mol. Physics* 26, 145-157 (1973).

3. L. Wolniewicz and K. Dressler, "The B $^1\Sigma_u^+$, B' $^1\Sigma_u^+$, C $^1\Pi_u$ states of the H_2 molecule. Matrix elements of angular and radial nonadiabatic coupling and improved *ab initio* potential energy curves," *J. Chem. Phys.* 88, 3861-3870 (1988).

4. S. T. Pratt, P. M. Dehmer, and J. L. Dehmer, "Constant-ionic-state spectroscopy of high-v Rydberg states of molecular hydrogen," *J. Chem. Phys.* 97, 3038-3049 (1992).

5. R. S. Berry, "Ionization of molecules at low energies," *J. Chem. Phys.* 45, 1228-1245 (1966).

6. J. N. Bardsley, "Ionization of molecules near threshold," *Chem. Phys. Lett.* 1, 229-232 (1967).

7. G. Herzberg and Ch. Jungen, "Rydberg series and ionization potential of the H_2 molecule," *J. Mol. Spectrosc.* 41, 425-486 (1972).

8. S. L. Anderson, G. D. Kubiak, and R. N. Zare, "Resonance-enhanced multiphoton ionization of molecular hydrogen via the E,F $^1\Sigma_g^+$ state: Photoelectron energy and angular distributions," *Chem. Phys. Lett.* 105, 22-27 (1984).

9. Calculated from the ionization potential of Ref. 10 and the dissociation energy of Ref. 11.

10. E. F. McCormack, J. M. Gilligan, C. Cornaggia, and E. E. Eyler, "Measurement of high Rydberg states and the ionization potential of H_2," *Phys. Rev. A* 39, 2260-2263 (1989).

11. L. Wolniewicz and T. Orlikowski, "The $1s\sigma_g$ and $2p\sigma_u$ states of the H_2^+, D_2^+, and HD^+ ions," *Mol. Phys.* 74, 103-111 (1991).

12. M. A. O'Halloran, P. M. Dehmer, F. S. Tomkins, S. T. Pratt, and J. L. Dehmer, "Vibrational branching ratios following two-color excitation of autoionizing np Rydberg states of H_2," *J. Chem. Phys.* 89, 75-84 (1988).

13. E. Y. Xu, A. P. Hickman, R. Kachru, T. Tsuboi, and H. Helm, "Photoelectron spectroscopy of vibrationally excited H_2 (E,F $^1\Sigma_g^+$)," *Phys. Rev. A* 40, 7031-7038 (1989).

14. S. T. Pratt, E. F. McCormack, J. L. Dehmer, and P. M. Dehmer, "Field-induced ion-pair formation in molecular hydrogen," *Phys. Rev. Lett.* 68, 584-587 (1992).

15. E. F. McCormack, S. T. Pratt, P. M. Dehmer, and J. L. Dehmer, "Dissociation dynamics of high-v Rydberg states of molecular hydrogen," *J. Chem. Phys.*, submitted.

END

DATE FILMED

3/19/93